IEEE Access
Multidisciplinary | Rapid Review | Open Access Journal

Received November 22, 2021, accepted December 11, 2021, date of publication December 22, 2021,
date of current version January 6, 2022.

*Digital Object Identifier 10.1109/ACCESS.2021.3137454*

# Triboelectric Energy Generation for Modulating the Intermodulation of Quartz Oscillators in a Transmitter-to-Receiver System

**WEN-TENG CHANG, CHENG-TING KUO, TING-HE SHEN, HUNG-SHIU LIN, AND YU-TING SU**
Department of Electrical Engineering, National University of Kaohsiung, Kaohsiung 811, Taiwan

Corresponding author: Wen-Teng Chang (wtchang@nuk.edu.tw)

The authors thank Harmony Electronics Corp. for providing the complimentary quartz crystal. The project is supported under contract number MOST 110-2221-E-390-013.

**ABSTRACT** A quartz oscillator has a stable frequency that can be tuned by applying a voltage across the quartz crystal. This study applied a triboelectric generator (TEG) as mechanical stimuli on the input voltage of a remote transmitter in a transmitter-to-receiver system. The intermodulation (IM) frequencies were chosen instead of the transmitter frequencies because the IM signals are generally significant. This study first examined the rectified electric voltage from contact-separation and single-electrode mode TEGs. The series connection TEG, stored capacitor, and passive voltage regulator (zener diode) determine the quality of the direct current voltage. The increase in the input voltage via mechanical stimuli on the transmitter was proved to deliver a signal where the IM frequencies increase with the stimuli in the system.

**INDEX TERMS** Triboelectric energy generation, energy harvesting, intermodulation, quartz oscillator.

## I. INTRODUCTION

Wearable devices generally require wireless communication to monitor mechanical stimuli. Health and activity monitoring devices demonstrate the superiority of self-powered mechanisms [1]–[4]. The need for energy harvesting may come from different sources in an ambient environment. Photovoltaic, thermoelectric, electromagnetic, piezoelectric, and triboelectric approaches are the most common technologies for ambient energy harvesting [3]–[21]. Some of the technologies may exhibit complex structures, high-frequency operation, low conversion efficiency, or low output voltage, which could limit their application in smart power supply. A triboelectric generator (TEG) may be a suitable technology that has been reported to have a relatively simple structure, high energy density, and low cost [18]–[21]. In addition, the flexibility of the structure indicates that TEG has potential application in the biomedical field [22].

The piezoelectric generator presents a self-powered approach to transmitting signals through mechanical stimuli on a remote sensing system [23]. TEGs also demonstrate a similar remote energy harvesting ability. Induction copper coils and commercial antennas powered by TEG provide wireless power and/or signal sources in a transmitter-to-receiver system [24], [25]. Light-emitting diodes powered by TEG can be used for signal transmission [26], [27]. Although many works applied self-powered approaches for signals to a transmitter-to-receiver system, few studies considered a quartz crystal (QC)-based oscillator as a transmitter-to-receiver system. A QC oscillator has high-quality and high-temperature stability, that is, it is highly accurate and has low energy dissipation. The frequency of a quartz oscillator is tunable by applying a voltage across the QC because QC is a piezoelectric material, thus making quartz oscillators an ideal media for wireless transmission [28], [29]. In addition, quartz oscillators for transmitters and receivers can be highly discernible distinguishable because their frequencies are dependent on QC and the frequencies are subject to the orientation of the QC cut. This research intended to apply different TEG modes through mechanical stimuli on the input voltage of the transmitter and also aims to examine the factors of the TEG circuit for the transmitter-to-receiver system.

## II. TRANSMITTER-TO-RECEIVER SYSTEM AND TRIBOELECTRIC ENERGY GENERATOR

The transmitter-to-receiver system uses the same quartz oscillators as the transmitter and receiver. The difference between the transmitter and receiver is that the receiver is

The associate editor coordinating the review of this manuscript and approving it for publication was Michail Kiziroglou.


This work is licensed under a Creative Commons Attribution 4.0 License. For more information, see https://creativecommons.org/licenses/by/4.0/

connected to a spectrum analyzer, whereas the transmitter is powered by mechanical stimuli through TEG. The number of transmitter and receiver can be expanded by adding the same quartz oscillators with different oscillation frequencies. Power mechanisms include contact-separation and single-electrode mode TEGs. Contact-separation (CS) mode TEGs generally generate a high-voltage pulse output with simple geometries [30]. In contrast, the single-electrode (SE) mode TEGs are constructed with only one triboelectric surface so that a human hand serves the other electrode, thus ensuring that the setup can integrate easily with other electronics [31].

### A. SCHEMATIC OF SIGNAL TRANSMISSION AND ENERGY GENERATOR

The transmitter-to-receiver system uses the near-field region because the frequencies of the commercial QC are operated in a low-frequency region in tens of MHz. In this region, the radiation distance (r) is relatively shorter than wavelength ($\lambda$). The reactive near-field has strong capacitive or inductive effects, thus being suitable for wireless powering [32], [33]. Then, the transmission causes a signal interference that shares the same space. The interference generates harmonic frequencies because of nonlinear features. However, if the operating and interference frequencies are well known, then this intermodulation (IM) can be reconstructed, thus converting the IM distortion for sensing purposes.

A quartz oscillator provides a stable oscillation frequency that depends mainly on the natural frequency of the QC. The IM signal ($S_i$) is composed of a transmitter signal ($S_t$) and a received signal ($S_r$). The nonlinear output spectrum ($S_o$) at the spectrum analyzer is expressed as follows:

$$S_o = \sum_{n=1}^{\infty} a_n S_i^n = \sum_{n=1}^{\infty} a_n (S_t \cos 2\pi f_t t + S_r \cos 2\pi f_r t)^n \quad (1)$$

where $a_n$ is an independent coefficient related to $S_i$. $f_r$ and $f_r$ are the fundamental frequencies of the receiver and transmitter, respectively. The natural frequency of the QC determines the fundamental frequencies of the quartz oscillator. The collapsing series in Eq. (1) results in the spectrum of frequencies m $\times f_r \pm$ n $\times f_t$, where m and n are integers. Although the infinite order of signal tones can be found on the spectrum, the power (amplitude) generally decreases with increasing order. In addition, the IM products are usually higher than pure transmission signals because the $S_r$ is significantly higher than $S_t$ when the spectrum is connected to the receiver side.

Fig. 1 shows the schematic of the interference of the transmitters and receiver and the necessary power in the transmitter-to-receiver system. The receiver can discriminate different sources of the frequencies from the transmitters because of their different frequencies. This work limited the self-powered unit for input voltage ($V_i$) supply (dashed box) to the transmitter side. The QC is a piezoelectric material that is used to tune the oscillation frequency (f+$\Delta$f) of the voltage-controlled oscillator (VCO) with $V_i$. The identities

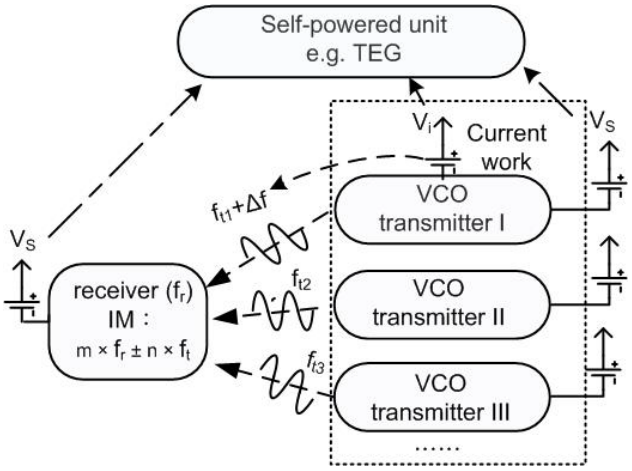


**FIGURE 1.** Schematic of multiple transmitters and a receiver made of VCOs. The input voltage ($V_i$) is powered by a self-powered unit, whereas the circuits ($V_S$) are supplied by a 9 V battery. The IM product of the frequencies of the receiver and transmitter (m × $f_r$± n × $f_t$) is applied, and the oscillation frequencies of the transmitters are tunable ($\Delta$f) through $V_i$. Notably, this work applied one transmitter.

of the transmitter and receiver are exchangeable because the oscillator circuits are the same. Although the circuits used external power ($V_s$), the circuits are likely powered by TEG [34]. In addition, the integrated circuit can save more power than the discrete circuits. The IM product of the frequencies of the receiver and transmitter (m × $f_r$± n × $f_t$) are preferable (m and n are integers) because IM signals are generally significant.

### B. TEG FOR VOLTAGE INPUT ON VCO

The working mechanism of TEG comes from the coupling of triboelectricity and electrostatic induction effects. When two different triboelectric materials contact each other and separate, electrons will flow back and forth through the external circuit to maintain balance because of the instantaneous voltage difference [1], [35]. Generally, the working mechanism of TEG has four modes: CS, in-plane sliding, SE, and free-standing mode [24], [35]. The energy density is related to the coupling of the dielectric polarization. Hence, the generation of electric current is related to the change of the capacitance (dC/dt) and voltage (dV/dt), which is as follows:

$$i = V\frac{dC}{dt} + C\frac{dV}{dt} \quad (2)$$

In addition to using the micro/nanosurface structure to improve the energy harvesting ability [1], the use of external charge pumping can achieve a high and stable output [36].

The mechanical energy to electrical energy in this work applies two different operating mechanisms. The first is CS mode TEG; a schematic of a pair of CS modes TEGs is shown in Fig. 2(a). A leaf-like TEG consists of a thin PET, aluminum foil electrode, polytetrafluoroethylene (PTFE) film, and a copper electrode. The electrode contacts stick to the PTFE films, and contact and separation cause the charge

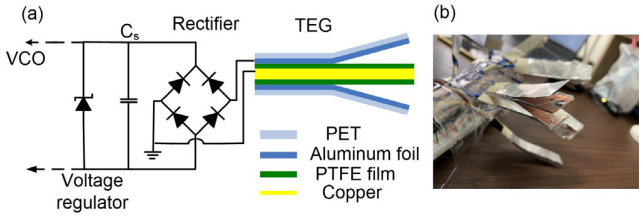


**FIGURE 2.** (a) Schematic of a pair of CS mode TEGs. A leaf-like TEG consists of a thin PET, aluminum foil electrode, PTFE film, and copper electrode. The contact and separation cause the charge to accumulate on two electrodes. The bridge rectifier converts the voltage signals into positive waveforms and is stored in the capacitor ($C_s$). The DC voltage connected to a VCO is regulated by a zener diode (voltage regulator). (b) Pairs of CS leaves. Each leaf is approximately 1.5 cm × 7.5 cm (1 cm bonding) in size.

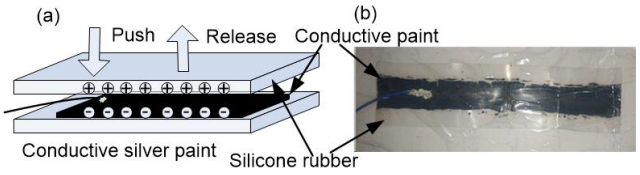


**FIGURE 3.** (a) Schematic of an SE mode TEG, which consists of conductive paint sandwiched by two pieces of silicone rubber. The push-and-release cycles applied by bare hands cause the charge accumulation. (b) SE mode TEG; the conductive paint is approximately 15 cm × 2 cm.

to accumulate on two electrodes. The bridge rectifier converts the voltage signals into positive waveforms. The potential difference decreases for the next contact. The capacitors ($C_s$) store the charges and feed them to the input of the oscillator. The frequency of the VCO transmitter changes with the input voltages, so the DC input voltages were regulated by replacing the zener diodes. Fig. 2(b) shows the photo of the pairs of leafs. Each leaf is approximately 1.5 cm × 7.5 cm (1 cm bonding) in size. The electric properties were recorded using a Tektronix DMM 6500 digital multimeter when tapping the leaf-like TEGs.

The other is the SE mode TEG, which was constructed with conductive paint with a thickness less than 1 mm, sandwiched by two pieces of silicone rubber with a thickness of 0.5 mm (Fig. 3(a)). The push-and-release cycles applied by bare hands cause the charge separation. Fig. 3(b) presents an image of the SE mode TEG. The conductive paint is approximately 15 cm × 2 cm.

### C. VCO FOR THE TRANSMITTER AND RECEIVER

The transmitter and receiver used the same oscillator circuit mounted on printed circuit boards powered by an independent 9 V battery to avoid IMs from the household power. The oscillator circuit consists of inverters (74IS04), 5 V voltage regulator (7805), and AT-cut QC (Fig. 4[a]). The natural frequencies of QCs on the receiver and the transmitter are 5.12 and 3.54 MHz, respectively. The receiver's output was connected to a spectrum analyzer (RIGOL DSA815), and the control terminal ($V_i$) of the transmitter was connected to the TEG. The transmitter's frequency is not only determined by the natural frequency of the QC but also tuned by $V_i$.

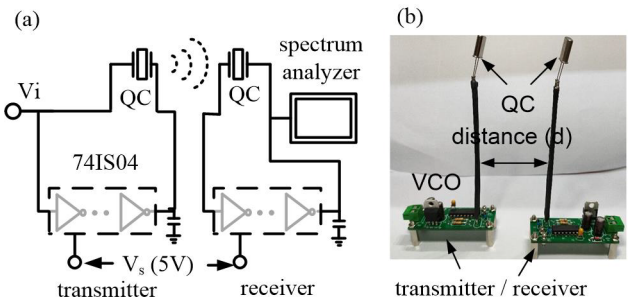


**FIGURE 4.** (a) Schematic of the oscillator used on the transmitter and receiver. The oscillator circuit consists of inverters, voltage regulators, and AT-cut QC. The receiver's output is connected to the spectrum analyzer, whereas the control terminal of the transmitter is connected to the TEG. (b) Transmitter and the receiver whose distance is d.

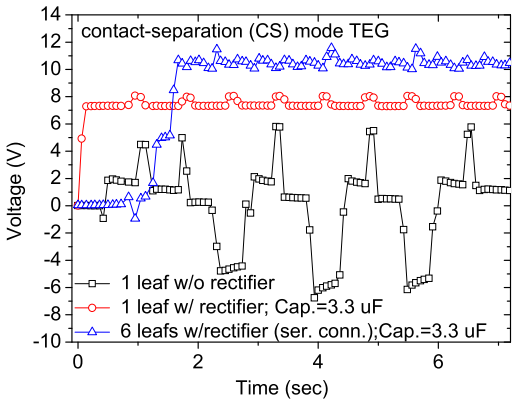


**FIGURE 5.** Open voltage generated by the CS mode TEG with 1 leaf-like TEG without a rectifier (square), 1 leaf-like TEG with a rectifier (circle), and 6 leaf-like TEGs with a rectifier (triangles).

A long antenna assists in receiving signals (Fig. 4[b]). The two oscillators are separate with a distance (d).

## III. RESULTS AND DISCUSSION

The mechanical stimuli via TEG intended to extract a constant DC voltage used on quartz-based VCO. Thus, this study focused on the DC voltage generated from the different modes of TEG and their rectifier circuits. Both the abovementioned CS and SE mode TEGs were applied to generate electrons that were then stored on a capacitor. The open voltage of the CS mode TEG was less sensitive to driving force, whereas the SE mode was sensitive to the driving force. As the capacitance of the capacitor is the ratio of the amount of maximum charge to the applied voltage, the ratio is related to the speed of the ascended voltage. The DC voltages were varied by replacing different passive voltage regulators (zener diodes) to observe the IM frequencies.

### A. RECTIFIER AND STORING CHARGE OF THE TEG POWER GENERATION

A rectifier is essential to obtain a stable voltage. With a tapping cycle of 2 s on a single leaf-like CS mode TEG, the output voltage appears positive and negative (Fig. 5). However, a full-wave rectifier and a capacitor (3.3 $\mu$F) kept

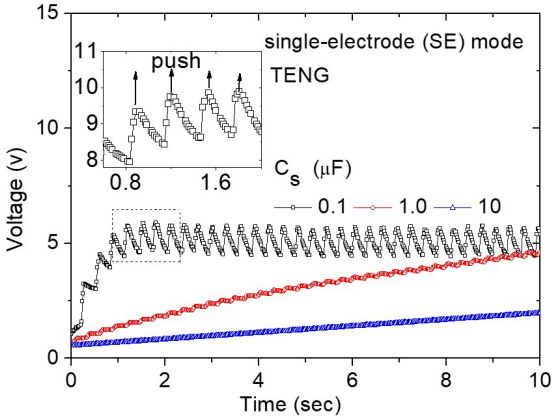


**FIGURE 6.** Open voltage generated by the SE mode TEG with a parallel capacitor ($C_S$) of 0.1 $\mu$F (square), 1 $\mu$F (circle), and 10 $\mu$F (triangle). The inset indicates that the ripple voltage changes with the tapping frequency ($C_S = 0.1\mu F$).

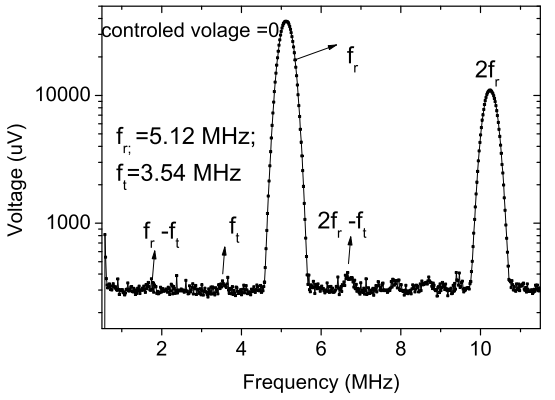


**FIGURE 7.** Logarithm scale of the spectrum on the receiver side that exhibits the harmonic frequencies of the receiver ($n \times f_r$), transmitter ($n \times f_t$), and the IMs, for example, $f_r - f_t$ and $2f_r - f_t$. The fundamental frequencies of the transmitter and receiver are 3.54 and 5.12 MHz, respectively. The distance between the receiver and transmitter here is 20 mm.

the voltage positive and stable. The series connection of the TEG enhances the output voltage up to 10 V.

A capacitor in the TEG circuit is used to store accumulated electrical charge. With about 0.5 N of finger tapping force, the SE mode TEG circuit with a smaller capacitor ($C_s$) exhibits a faster charging voltage (Fig. 6). However, the connection with a small $C_s$ (0.1 $\mu$F) presents more ripples than those with a large $C_s$(1 and 10 $\mu$F). The rising voltage and accumulated charge also depend on the pressing frequency (inset, Fig. 6). Each press increases the charging voltage, whereas the voltage drops when tapping stops.

### B. CHARACTERIZATION OF IM OF REMOTE VCO

Fig. 7 shows the nonlinear features of the oscillator circuit with the interference of the receiver and transmitter. The figure includes their harmonics and IMs. The harmonic frequencies on the receiver side (integer multiples (n) of the fundamental frequency; $n \times f_t$) exhibit the maximum amplitude because the spectrum analyzer is directly connected

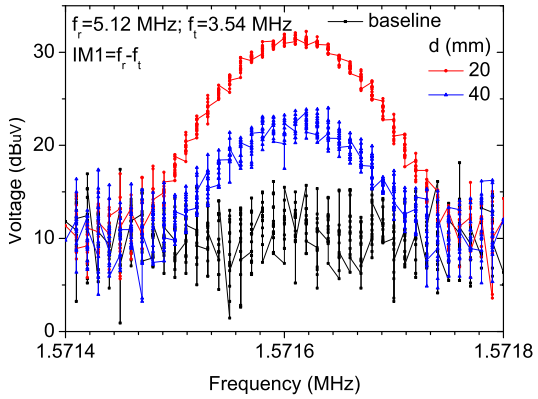


**FIGURE 8.** First-order IM ($f_r$-$f_t$) for the transmitter-to-receiver distances of 20 mm, 40 mm, and the baseline. The QC frequencies on the transmitter ($f_t$) and the receiver ($f_r$) are 3.54 and 5.12 MHz, respectively.

to the receiver. Unlike the amplitude (power) of the receiver, that of the transmitter at the harmonic frequencies ($n \times f_t$) depends on the distance. The product of two signals to generate IM signals at the frequencies of $m \times f_r \pm n \times f_t$ could be preferable to the harmonic signals of the transmitter.

To study the power transfer from the transmitter to the receiver, Fig. 8 depicts the first-order IM ($IM1 = f_r - f_t$) with the distance (d) of 20 mm, 40 mm, and the baseline (without IM). The transfer voltage is roughly proportional to the reciprocal of the d. The power (radiant flux) is proportional to the square of the voltage. The energy flux of the electromagnetic field is proportional to the inverse square of the distance (d) on the basis of the Poynting vector [37]. This result is similar to a previous report [28].

### C. TRIBOELECTRIC GENERATOR (TEG) FOR VOLTAGE INPUT ON VCO

One of the significant benefits of using TEG for energy harvesting is its simple and accessible structure for constructing a flexible and wearable self-powered system. This study presented the feasibility of using SE and CS mode TEGs, which are applicable for voltage input on a remote signal transmitter. The modulated frequency of a VCO is dependent on the voltage input, which is why passive voltage regulators (zener diodes) that take no power were used for different DC voltages.

Fig. 9 shows the third-order IM (IM3) frequency with no voltage input and with voltage inputs of 2, 2.5, and 5 V by replacing different zener diodes. Notably, the actual voltages input ($V_i$) are smaller than zener voltages. The frequency of a quartz oscillator can be modulated by the input DC voltage. Thus, the IM3 frequency increases with the increase in the input voltages by replacing different types of the zener voltage regulator on the transmitter. Fig. 10 shows the IM3 frequency with no voltage input and the voltage input of 2.5 V by the SE mode TEG. The experiment is similar to that conducted for the CS mode TEG except the current experiment used a small capacitor (0.1 $\mu$F). The frequency shift is 350 Hz, which is more significant than that in the

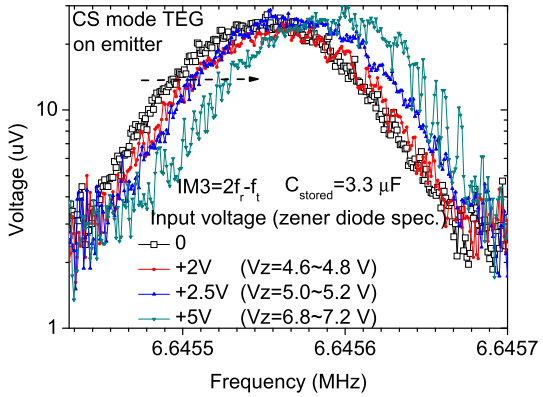


**FIGURE 9.** Third-order IM frequency (IM3 = $2f_r - f_t$) without controlled voltage (empty square) and with controlled voltage. The frequencies of IM3 increase with the increasing controlled voltages of 2, 2.5, and 5 V. The controlled voltages were supplied by the CS mode TEG and regulated by different zener diodes on the transmitter side.

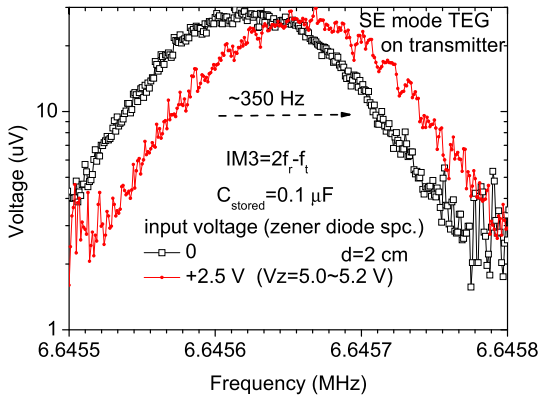


**FIGURE 10.** Frequencies of the third-order IM (IM3 = $2f_r - f_t$) without a controlled voltage (empty square) and with a controlled voltage input of 2.5 V. The controlled voltage of the transmitter was supplied by the SE mode TEG and regulated by a zener diode. A small capacitor of 0.1 $\mu$F is parallel connected.

situation where a capacitor of 3.3 $\mu$F was used under a 2.5 V voltage input.

## IV. CONCLUSION

This study presents the results of using a self-powered circuit for remote signal transmission. The TEG can independently serve as an energy source for voltage input for the VCO. The transmitter-to-receiver system can detect the remote mechanical stimuli through IM. Although the circuit's power supply still relied on an external source, a proper TEG design and an integrated circuit instead of a discrete circuit may satisfy the power consumption in a transmitter. For example, a low-power triple inverter (SN 74AUP3G04) requires 3.3 V and 20 mA operation, which is substantially smaller than what a typical triboelectric nanogenerator can provide [17]. This feature could enable the quartz oscillator-based transmitter-to-receiver system to serve a wireless self-powered machine, such as that for health monitoring. However, the oscillation frequency of the quartz oscillator is susceptible to a variety of factors, such as voltage supply, antenna configuration, near-field inductive coupling, and the orientation of quartz [28], [29]. The difference of the IM frequency without controlled voltage in Figures 9 and 10 may likely be attributed to the voltage supply [38]. A proper design to eliminate the deviation is required for further application. However, the current design exhibits a potential application where the roles of transmitters and receivers are interchangeable, and the transmitter's identity is recognizable when the frequencies of the QC are discernible.

## REFERENCES

[1] P.-K. Yang, L. Lin, F. Yi, X. Li, K. C. Pradel, Y. Zi, C.-I. Wu, J.-H. He, Y. Zhang, and Z. L. Wang, "A flexible, stretchable and shape-adaptive approach for versatile energy conversion and self-powered biomedical monitoring," *Adv. Mater.*, vol. 27, no. 25, pp. 3817–3824, May 2015.

[2] Q. Shi, H. Wang, T. Wang, and C. Lee, "Self-powered liquid triboelectric microfluidic sensor for pressure sensing and finger motion monitoring applications," *Nano Energy*, vol. 30, pp. 450–459, Dec. 2016, doi: 10.1016/j.nanoen.2016.10.046.

[3] K. Meng, S. Zhao, Y. Zhou, Y. Wu, S. Zhang, Q. He, X. Wang, Z. Zhou, W. Fan, X. Tan, J. Yang, and J. Chen, "A wireless textile-based sensor system for self-powered personalized health care," *Matter*, vol. 2, no. 4, pp. 896–907, Apr. 2020, doi: 10.1016/j.matt.2019.12.025.

[4] R. Sun, S. Carreira, Y. Chen, and C. Xiang, "Stretchable piezoelectric sensing systems for self-powered and wireless health monitoring," *Adv. Mater. Technol.*, vol. 4, no. 5, Feb. 2019, Art. no. 1900100, doi: 10.1002/admt.201900100.

[5] H. Liu, B. W. Soon, N. Wang, C. J. Tay, C. Quan, and C. Lee, "Feasibility study of a 3D vibration-driven electromagnetic MEMS energy harvester with multiple vibration modes," *J. Micromech. Microeng.*, vol. 22, no. 12, Nov. 2012, Art. no. 125020, doi: 10.1088/0960-1317/22/12/125020.

[6] L. Dhakar, F. E. H. Tay, and C. Lee, "Investigation of contact electrification based broadband energy harvesting mechanism using elastic PDMS microstructures," *J. Micromech. Microeng.*, vol. 24, no. 10, Sep. 2014, Art. no. 104002, doi: 10.1088/0960-1317/24/10/104002.

[7] H. Liu, S. Zhang, and T. Kobayashi, "Flow sensing and energy harvesting characteristics of a wind-driven piezoelectric Pb(Zr0.52, Ti0.48)$O_3$ microcantilever," *Micro. Nano. Lett.*, vol. 9, pp. 286–289, Apr. 2014, doi: 10.1049/mnl.2013.0750.

[8] H. Askari, A. Khajepour, and M. B. Khamesee, "Piezoelectric and triboelectric nanogenerators: Trends and impacts," *Nano Today*, vol. 22, pp. 10–13, Oct. 2018, doi: 10.1016/j.nantod.2018.08.001.

[9] B. Yang and C. Lee, "A wideband electromagnetic energy harvester for random vibration sources," *Adv. Mater. Res.*, vol. 74, pp. 165–168, Jun. 2009, doi: 10.4028/www.scientific.net/AMR.74.165.

[10] H. Liu, C. Lee, and T. Kobayashi, "Investigation of a MEMS piezoelectric energy harvester system with a frequency-widened-bandwidth mechanism introduced by mechanical stoppers," *Smart Mater. Struct.*, vol. 21, Mar. 2012, Art. no. 035005, doi: 10.1088/0964-1726/21/3/035005.

[11] Q. Shi, T. Wang, and C. Lee, "MEMS based broadband piezoelectric ultrasonic energy harvester (PUEH) for enabling self-powered implantable biomedical devices," *Sci. Rep.*, vol. 6, Apr. 2016, Art. no. 24946, doi: 10.1038/srep24946.

[12] Z. W. Yang, Y. Pang, and L. Zhang, "Tribotronic transistor array as an active tactile sensing system," *ACS Nano*, vol. 10, pp. 10912–10920, Nov. 2016, doi: 10.1021/acsnano.6b05507.

[13] Z. L. Wang, "On the first principle theory of nanogenerators from Maxwell's equations," *Nano Energy*, vol. 68, Feb. 2020, Art. no. 104272, doi: 10.1016/j.nanoen.2019.104272.

[14] M. Han, X. Zhang, and H. Zhang, *Flexible and Stretchable Triboelectric Nanogenerator Devices Toward Self-Powered Systems*, vol. 1. Hoboken, NJ, USA: Wiley, 2019.

[15] J. Chen, H. Guo, and C. Hu, "Robust triboelectric nanogenerator achieved by centrifugal force induced automatic working mode transition," *Adv. Energy Mater.*, vol. 10, no. 3, May 2020, Art. no. 2000886, doi: 10.1002/aenm.202000886.

[16] G. Yao, L. Xu, and X. Cheng, "Bioinspired triboelectric nanogenerators as self-powered electronic skin for robotic tactile sensing," *Adv. Funct. Mater.*, vol. 30, no. 6, pp. 1–9, Nov. 2019, doi: 10.1002/adfm.201907312.

[17] L. Gu, N. Cui, L. Cheng, Q. Xu, S. Bai, M. Yuan, W. Wu, and J. Liu, "Flexible fiber nanogenerator with 209 V output voltage directly powers a light-emitting diode," *Nano Lett.*, vol. 1, pp. 91–94, Dec. 2013, doi: 10.1021/nl303539c.

[18] Y. Yang, Z. Lin, T. Hou, F. Zhang, and Z. L. Wang, "Nanowirecomposite based flexible thermoelectric nanogenerators and self-powered temperature sensors," *Nano Res.*, vol. 5, pp. 888–895, Nov. 2012, doi: 10.1007/s12274-012-0272-8.
[19] C. He, W. Zhu, B. Chen, L. Xu, T. Jiang, C. B. Han, G. Q. Gu, D. Li, and Z. L. Wang, "Smart floor with integrated triboelectric nanogenerator as energy harvester and motion sensor," *ACS Appl. Mater. Interface*, vol. 9, no. 31, pp. 26126–26133, Jul. 2017, doi: 10.1021/acsami.7b08526.
[20] Y. Bai, L. Xu, S. Lin, J. Luo, H. Qin, and K. Han, "Charge pumping strategy for rotation and sliding type triboelectric nanogenerators," *Adv. Energy Mater.*, vol. 10, no. 21, Apr. 2020, Art. no. 2000605, doi: 10.1002/aenm.202000605.
[21] L. Dhakar, F. E. H. Tay, and C. Lee, "Development of a broadband triboelectric energy harvester with SU-8 micropillars," *J. Microelectromech. Syst.*, vol. 24, no. 1, pp. 91–99, Feb. 2015, doi: 10.1109/JMEMS.2014.2317718.
[22] X.-S. Zhang, M. Han, B. Kim, J.-F. Bao, J. Brugger, and H. Zhang, "All-in-one self-powered flexible microsystems based on triboelectric nanogenerators," *Nano Energy*, vol. 47, pp. 410–426, May 2018, doi: 10.1016/j.nanoen.2018.02.046.
[23] H. Nishikawa, A. Yoshimi, and K. Takemura, "Batteryless wireless transmission system for electronic drum uses piezoelectric generator for play signal and power source," *J. Phys., Conf.* vol. 660, Dec. 2015, Art. no. 012100.
[24] C. Zhang, "Conjunction of triboelectric nanogenerator with induction coils as wireless power sources and self-powered wireless sensors," *Nature Commun.*, vol. 11, Jan. 2020, Art. no. 58, doi: 10.1038/s41467-019-13653-W.
[25] A. Chandrasekhar, N. Alluri, and M. Sudhakaran, "A smart mobile pouch as a biomechanical energy harvester towards self-powered smart wireless power transfer applications," *Nanoscale*, vol. 9, p. 9818, Oct. 2017, doi: 10.1039/c7nr00110j.
[26] W. Ding, C. Wu, Y. Zi, H. Zou, J. Wang, J. Cheng, A. C. Wang, and Z. L. Wang, "Self-powered wireless optical transmission of mechanical agitation signals," *Nano Energy*, vol. 47, pp. 566–572, May 2018, doi: 10.1016/j.nanoen.2018.03.044.
[27] X. Liu, X. Wei, L. Guo, Y. Liu, Q. Song, and A. Jamalipour, "Turning the signal interference into benefits: Towards indoor self-powered visible light communication for IoT devices in industrial radio-hostile environments," *IEEE Access*, vol. 7, pp. 24978–24989, 2019, doi: 10.1109/ACCESS.2019.2900696.
[28] W. T. Chang and S. H. Lai, "Measuring reactive near-field interference using the quartz oscillators intermodulation," in *Proc. ECMSM*, Liberec, Czech Republic, Jun. 2015, pp. 1–4, doi: 10.1109/ECMSM.2015.7208678.
[29] W. T. Chang, K. J. Tseng, and S. H. Lai, "Electromagnetic intermodulation interference using quartz oscillators," in *Proc. IFCS*, Taipei, Taiwan, May 2014, pp. 1–5, doi: 10.1109/FCS.2014.6859934.
[30] X.-S. Zhang, M. Su, J. Brugger, and B. Kim, "Penciling a triboelectric nanogenerator on paper for autonomous power MEMS applications," *Nano Energy*, vol. 33, pp. 393–401, Mar. 2017, doi: 10.1016/j.nanoen.2017.01.053.
[31] B. Meng, W. Tang, Z. Too, X. Zhang, and M. Han, "A transparent single-friction-surface triboelectric generator and self-powered touch sensor," *Energy Environ. Sci.*, vol. 6, no. 11, pp. 3235–3240, 2013, doi: 10.1039/C3EE42311E.
[32] J. A. Paradiso and T. Starner, "Energy scavenging for mobile and wirelesselectronics," *IEEE Pervasive Comput.*, vol. 4, no. 4, pp. 18–27, Jan./Mar. 2005, doi: 10.1109/MPRV.2005.9.
[33] S. S. Valtchev, E. N. Baikova, and L. R. Jorge, "Electromagnetic field as the wireless transporter of energy," *Facta Univ. Ser. Electr. Eng.*, vol. 25, pp. 171–181, Oct. 2012, doi: 10.2298/FUEE1203171V.
[34] H. Wu, S. Wang, Z. Wang, and Y. Zi, "Achieving ultrahigh instantaneous power density of 10 MW/m$^2$ by leveraging the opposite-charge-enhanced transistor-like triboelectric nanogenerator (OCT-TENG)," *Nature Commun.* vol. 12, Sep. 2021, Art. no. 5470, doi: 10.1038/s41467-021-25753-7.
[35] Z. L. Wang and A. C. Wang, "On the origin of contact-electrification," *Mater. Today*, vol. 30, pp. 34–51, Nov. 2019, doi: 10.1016/j.mattod.2019.05.016.
[36] M. Li, W.-Y. Cheng, Y.-C. Li, H.-M. Wu, Y.-C. Wu, H.-W. Lu, S.-L. Cheng, L. Li, K.-C. Chang, H.-J. Liu, Y.-F. Lin, L.-Y. Lin, and Y.-C. Lai, "Deformable, resilient, and mechanically-durable triboelectric nanogenerator based on recycled coffee waste for wearable power and self-powered smart sensors," *Nano Energy*, vol. 79, Jan. 2021, Art. no. 105405, doi: 10.1016/j.nanoen.2020.105405.
[37] J. Blumenthal, F. Reichenbach, and D. Timmermann, "Minimal transmission power vs. signal strength as distance estimation for localization in wireless sensor networks," in *Proc. 3rd Annu. Commun. Soc. Sensor Ad Hoc Commun. Netw.*, Sep. 2006, pp. 761–766, doi: 10.1109/SAHCN.2006.288558.
[38] T. Wu, K. Mayaram, and U.-K. Moon, "An on-chip calibration technique for reducing supply voltage sensitivity in ring oscillators," *IEEE J. Solid-State Circuits*, vol. 42, no. 4, pp. 775–783, Apr. 2007, doi: 10.1109/JSSC.2007.892194.

**WEN-TENG CHANG** received the B.S. degree in electrical engineering from the National Tsing Hua University, Hsinchu, Taiwan, in 1994, and the M.S. and Ph.D. degrees in electrical engineering and computer science from Case Western Reserve University, Cleveland, OH, USA, in 2004 and 2006, respectively. He joined Applied Materials, Taiwan, and Chi Mei Optoelectronics, in 1997 and 1999, respectively. In 2006, he joined as a Faculty Member at the National University of Kaohsiung, Kaohsiung, Taiwan, where he became an Associate Professor and a Professor with the Department of Electrical Engineering, in 2010 and 2013, respectively. His current research interests include field emission devices, renewable energy, and advanced semiconductor transistors.

**CHENG-TING KUO** is currently pursuing the B.S. degree in electrical engineering with the National University of Kaohsiung, Kaohsiung, Taiwan. His contributions in this work include the intermodulation distortion of quartz oscillator and related wireless signal transmission.

**TING-HE SHEN** was born in 2000. He is currently pursuing the B.S. degree in electrical engineering with the National University of Kaohsiung, Kaohsiung, Taiwan. His work included the function of the single-electrode mode triboelectric generator.

**HUNG-SHIU LIN** is currently pursuing the B.S. degree in electrical engineering with the National University of Kaohsiung, Kaohsiung, Taiwan. Since 2020, he has been investigating the application of static electricity, particularly on the contact-separation mode triboelectric generators.

**YU-TING SU** is currently pursuing the B.S. degree in electrical engineering with the National University of Kaohsiung, Kaohsiung, Taiwan. Her research interest includes voltage controlled oscillator using quartz oscillator for wireless signal transmission.